ISSN 0869-5911, Petrology, 2008, Vol. 16, No. 6, pp. 552–564. © Pleiades Publishing, Ltd., 2008.
Original Russian Text © A.A. Borisov, 2008, published in Petrologiya, 2008, Vol. 16, No. 6, pp. 593–605.

Experimental Investigation of K and Na Partitioning between Miscible Liquids

A. A. Borisov

Institute of Geology of Ore Deposits, Petrography, Mineralogy, and Geochemistry, Russian Academy of Sciences, Staromonetnyi 35, Moscow, 119017 Russia

e-mail: aborisov@igem.ru

Received August 28, 2007; in final form, November 21, 2007

Abstract—Model silicate melts with variable Al_2O_3 and SiO_2 contents were experimentally saturated with alkalis at a total pressure of 1 atm and temperatures of 1300–1470°C, using the crucible supported loop technique. It was shown that Al_2O_3 content has little influence on the degree of silicate melt saturation with K and Na. In contrast, SiO_2 content strongly affects the solubility of alkalis in silicate melts. Model calculations were performed to evaluate the behavior of alkalis during the contamination/mixing of basic and silicic magmas.

DOI: 10.1134/S0869591108060027

INTRODUCTION

The investigation of component partitioning between immiscible liquids usually does not pose technical problems, although special experimental designs may be helpful even in this case (Veksler et al., 2006). At first glance, the investigation of the equilibrium partitioning of alkalis between *miscible* melts seems to be impossible. In such a case, experimental efforts are limited to the analysis of diffusion zoning at the boundary between touching miscible melts (e.g., basalt/granite; Watson and Jurewicz, 1984). Meanwhile, the results of such investigations are essential for the analysis of probable changes in melt composition due to the crustal contamination of ascending magmas, metasomatism of xenoliths in kimberlites and alkali basalts, etc.

Wall rock assimilation by magmas was considered in detail in the pioneering study of Bowen (1928). Nowadays, it is universally accepted that basaltic magmas passing through a thick continental crust can hardly reach the surface without assimilating wall rocks to some degree.

The experimental studies that are (or could be) used to tackle the problem of magma contamination and mixing can be subdivided into three groups.

(1) The investigation of the dissolution of crystalline phases (primarily quartz) in basaltic melts (Sato, 1975; Watson, 1982). Experiments of this group provide insight into the rate and character of dissolution of the main minerals of the felsic crust in basaltic melts. It is in such experiments that uphill diffusion of alkalis, i.e., diffusion of elements against their concentration gradients, was revealed by the microprobe examination of a thin layer of silicic melt around quartz grains.

(2) The analysis of component partitioning between immiscible liquids (Watson, 1976; Ryerson and Hess, 1978; Hess and Wood, 1982; etc.). The advantage of this method is the reliable determination of partition coefficients for minor elements between basic (iron-rich) and silicic melts. Its shortcoming is the restriction to the systems exhibiting liquid immiscibility (i.e., simplified systems) and often at relatively low temperatures (below 1200°C).

(3) Finally, most experimental work has probably focused on the interaction of contacting silicic (granite, dacite, and rhyolite) and basic (basalt) melts at high temperatures and pressures (Yoder, 1973; Watson, 1982; Watson and Jurewicz, 1984; Kouchi and Sunagawa, 1985; Johnston and Wyllie, 1988; Bindeman and Perchuk, 1993; etc.). Depending on the experimental temperature, the contrasting composition may be partly or completely melted. This method is advantageous in that it can be used to study natural compositions, which undoubtedly facilitates the extrapolation of results obtained in small ampoules and relatively short experiments to large volumes and times.

In the context of our study, of special importance is that experiments on the interaction of contrasting melts demonstrated higher mobility of alkalis compared with other melt components (e.g., Si^{4+} and Al^{3+}). Watson (1982) introduced the concept of "transient two-liquid equilibrium" for such systems. He also supposed that the transient partition coefficients of alkalis between basaltic and silicic melts should qualitatively resemble the stable partition coefficients of alkalis between immiscible basic and silicic liquids. The values of transient partition coefficients must control the direction of alkali diffusion between the contrasting melts. The need to use diffusion profile is perhaps the only shortcoming of this approach.

In this paper we report experimental results on the partitioning of sodium and potassium between several

miscible liquids obtained by the crucible supported loop technique (Borisov et al., 2006) and discuss the problems of magma contamination and mixing.

EXPERIMENTAL METHODS

Experiments were carried out using a vertical tube furnace at the Institut für Geologie und Mineralogie, Universität zu Köln (Germany). Oxygen fugacity was controlled by a $CO–CO_2$ gas mixture and calculated from the proportions of gases under experimental temperatures using the tables of Deines et al. (1974). Temperature in the working zone of the furnace was measured by a $PtRh_6–PtRh_{30}$ thermocouple calibrated against the melting points of pure Au (1064°C) and Ni (1453°C). The uncertainties of the determination of temperature and $\log f_{O_2}$ were no higher than ±2°C and ±0.2, respectively.

It was supposed that, other factors being equal, the degree of melt saturation in alkalis, which are very strong network modifiers, is controlled primarily by the content of network-forming oxides. Therefore, two systems were selected for experiments: with variable Al_2O_3 and variable SiO_2 contents.

The first system was based on the $2CaO \cdot 3SiO_2$ (moles) melt modified by the addition of various amounts of Al_2O_3 (compositions CSA6, CSA12, CSA18, and CSA25 in Table 1). The second model system was based on the eutectic composition of the anorthite–diopside system (DA), which was modified by adding various amounts of SiO_2 (compositions DA, DAS25, DAS50, DAS70, DAS100, DAS200, and DAS400 in Table 1). Some compositions of the second system were previously used by us for the investigation of the influence of silica content in the melt on the solubility of nickel, cobalt, and iron (Borisov, 2006, 2007).

Experiments were carried out by the crucible supported loop technique (Borisov et al., 2006), which is illustrated in Fig. 1 in a modification for the simultaneous investigation of several melts. The essence of the method is as follows. A small quartz crucible (15 mm inner diameter and 22 mm height) is filled by one-third with an alkali-rich melt of the $SiO_2 \pm Na_2O \pm K_2O$ composition, which serves subsequently as a source of Na and/or K vapors. Up to five loops of Pt wire (0.15 mm in diameter) with the mixtures of interest (up to 3 mm in diameter) are suspended above the melt under a platinum lid. The crucible is lowered into the furnace and held under desired $T–f_{O_2}$ parameters for several hours. During the experiment, the initially alkali-free compositions in the loops are affected by alkali vapor and, thus, become simultaneously saturated with alkalis. The experimental conditions are shown in Table 2.

Note that the ideology of the crucible supported loop technique is similar to the approach proposed by O'Neill (2005). In that case, a large Pt crucible with a source melt was placed in a furnace approximately 10 cm beneath samples, which produced a certain partial pressure of alkali vapors in the working zone of the furnace.

Table 1. Compositions of starting glasses, wt %

Composition	SiO_2	Al_2O_3	MgO	CaO
$Ca_2Si_3O_8–Al_2O_3$ system				
CSA6	57.8	6.7	–	35.5
CSA12	53.7	13.3	–	32.9
CSA18	49.7	19.9	–	30.3
CSA25	45.6	26.7	–	27.7
An–Di eutectic–SiO_2 system				
DA	50.2	15.7	10.3	23.7
DAS25	58.5	13.2	8.6	19.7
DAS50	66.8	10.5	6.9	15.8
DAS70	70.4	9.4	6.2	14.1
DAS100	75.0	7.9	5.2	11.9
DAS200	83.0	5.4	3.5	8.1
DAS400	90.8	2.8	1.9	4.5

Note: The compositions are average microprobe analyses of all experimental glasses (Table 3) recalculated to alkali-free compositions.

At first glance, oxygen fugacity should play no role in experiments with iron-free melts. However, it is known that alkali loss from a melt increases considerably under reduced conditions (Donaldson et al., 1975; Corrigan and Gibb, 1979). This indicates that the pressure of alkali vapor above the melt increases with decreasing oxygen fugacity. By varying f_{O_2} values in our experiments, we managed to increase or decrease the partial pressure of alkali vapors in the crucible, which resulted in different levels of melt saturation with Na_2O and K_2O at a given temperature. After being held at the desired temperature and oxygen fugacity, the samples were quenched in the upper cold zone of the furnace.

Quenched glasses were analyzed using a JEOL Superprobe electron microprobe at the Institut für Geologie und Mineralogie, Universität zu Köln (Germany). Natural albite, orthoclase, corundum, and diopside were used as standards. In most cases, the accelerating voltage was 15 kV; beam current, 15 nA; and counting time, 40 s. From 10 to 20 spots were analyzed in each sample. The mean compositions of experimental glasses in the CSA and DAS systems are given in Table 3.

The hygroscopic glasses that were used as reservoirs for alkalis were polished with alcohol as a lubricant and analyzed with a defocused electron beam (20 μm) at a

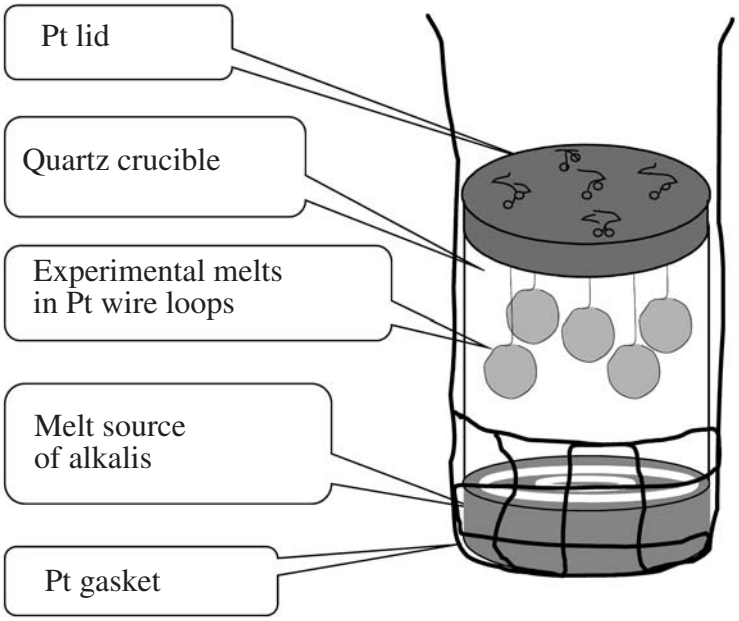

Fig. 1. Cartoon illustrating the arrangement of samples in the crucible supported loop technique. See text for further explanation.

counting time of 6 s. Similar to our previous study (Borisov et al., 2006), a small heterogeneity was observed in the source glasses from the meniscus to the crucible bottom. In order to compare glasses from different experiments, Table 2 reports the compositions of the upper parts of the cylinders (1 mm deep from the meniscus; average of 20–40 spot analyses).

EXPERIMENTAL RESULTS

Problem of Equilibration in Experiments on Melt Saturation with Na and K through a Vapor Phase

As can be seen from Table 2, the composition of melt that was used as an alkali source changed during the experiment toward a higher silica content owing to

Table 2. Experimental conditions and the compositions of melts that were used as alkali sources in the crucible supported loop technique

Series no.	Sample label	$-\log f_{O_2}$	Duration, h	Source label	Initial composition of the source, wt %				Final composition of the source, wt %			
					SiO_2	Na_2O	K_2O	Total	SiO_2	Na_2O	K_2O	Total
3	CSA_iNa-3	8.91	3.0	N2S-3	65.3	33.9	–	99.2	79.4	20.8	–	100.3
4	CSA_iNa-4	0.68	3.0	N2S-4	65.3	33.9	–	99.2	77.6	22.7	–	100.3
5	CSA_iNa-5	6.89	3.0	N2S-5	65.3	33.9	–	99.2	77.8	22.4	–	100.2
6	CSA_iNa-6	2.84	3.0	N2S-6	65.3	33.9	–	99.2	78.2	22.6	–	100.8
8	DANa-8, DAS_iNa-8	10.71	3.0	N2S-8	65.3	33.9	–	99.2	78.8	22.1	–	100.9
13	DANa-13, DAS_iNa-13	8.92	16.5	N4S-13	82.7	16.9	–	99.6	88.7	11.2	–	99.9
23	DAK-23, DAS_iK-23*	8.92	16.0	K2S-23	48.9	–	51.1	100.0	88.9	–	10.1	98.9
24	DAK-24, DAS_iK-24	8.93	16.0	K4S-24	76.3	–	22.2	98.5	85.9	–	13.1	99.0
25	CSA_iK-25	8.93	7.5	K4S-25	76.3	–	22.2	98.5	84.3	–	16.0	100.3
26	DANK-26, DAS_iNK-26	8.93	16.0	NKS-26	75.7	10.1	13.3	99.1	85.7	5.4	7.7	98.8
27	DANK-27, DAS_iNK-27	10.74	22.0	NKS-27	75.7	10.1	13.3	99.1	80.8	8.5	11.0	100.2

Note: All experiments were carried out at a temperature of 1470°C, except for series 27 (1300°C).

* The initial composition was calculated because the very high K_2O content in the melt source resulted in the fusion of the crucible bottom.

Table 3. Compositions of experimental glasses, wt %

Sample	SiO_2	Al_2O_3	MgO	CaO	Na_2O	s.d.	K_2O	s.d.	Total
$Ca_2Si_3O_8$–Al_2O_3 system, samples enriched in Na									
CSA6Na-3	53.80	6.30	–	33.55	6.69	0.11	–	–	100.34
CSA12Na-3	50.19	12.58	–	31.18	6.78	0.15	–	–	100.73
CSA18Na-3	46.17	18.75	–	28.79	6.87	0.13	–	–	100.58
CSA25Na-3	42.58	25.12	–	26.48	6.84	0.11	–	–	101.02
CSA6Na-4	56.50	6.54	–	34.86	2.08	0.08	–	–	99.99
CSA12Na-4	52.99	13.34	–	32.53	1.85	0.06	–	–	100.71
CSA18Na-4	49.06	19.90	–	30.04	1.62	0.07	–	–	100.63
CSA25Na-4	45.32	26.65	–	27.65	1.33	0.06	–	–	100.94
CSA6Na-5	54.69	6.27	–	33.11	5.71	0.13	–	–	99.78
CSA12Na-5	50.70	12.54	–	30.81	5.76	0.08	–	–	99.82
CSA18Na-5	47.10	18.85	–	28.43	5.84	0.10	–	–	100.22
CSA25Na-5	43.20	25.23	–	25.90	6.07	0.10	–	–	100.41
CSA6Na-6	56.57	6.53	–	34.69	1.33	0.04	–	–	99.11
CSA12Na-6	52.79	13.06	–	32.00	1.77	0.06	–	–	99.62
CSA18Na-6	48.81	19.64	–	29.57	1.75	0.08	–	–	99.77
CSA25Na-6	45.43	26.65	–	26.92	1.51	0.06	–	–	100.50
$Ca_2Si_3O_8$–Al_2O_3 system, samples enriched in K									
CSA6K-25	54.64	6.18	–	33.26	–	–	5.73	0.09	99.81
CSA12K-25	50.65	12.33	–	31.05	–	–	5.88	0.08	99.91
CSA18K-25	46.84	18.31	–	28.38	–	–	5.84	0.08	99.38
CSA25K-25	42.56	24.31	–	25.92	–	–	6.43	0.10	99.22
An-Di eutectic–SiO_2 system, samples enriched in Na									
DANa-8	46.93	14.83	9.70	22.28	6.47	0.10	–	–	100.20
DAS25Na-8	53.22	12.01	7.87	17.99	9.52	0.14	–	–	100.60
DAS50Na-8	59.05	9.47	6.18	14.07	11.57	0.13	–	–	100.34
DAS70Na-8	62.14	8.29	5.43	12.36	12.52	0.17	–	–	100.74
DANa-13	47.25	14.86	9.69	22.42	5.58	0.10	–	–	99.80
DAS25Na-1	53.81	12.10	7.91	18.18	8.07	0.12	–	–	100.07
DAS50Na-13	60.02	9.50	6.24	14.22	9.98	0.15	–	–	99.96
DAS100Na-13	66.26	7.14	4.68	10.69	11.02	0.16	–	–	99.79
DAS200Na-13	73.50	4.72	3.16	7.15	11.56	0.12	–	–	100.08
An-Di eutectic–SiO_2 system, samples enriched in K									
DAK-23	48.17	14.89	9.84	22.65	–	–	5.47	0.09	101.03
DAS100K-23	65.38	6.80	4.58	10.67	–	–	13.01	0.11	100.44
DAS200K-23	71.68	4.70	2.97	7.02	–	–	13.83	0.17	100.20
DAS400K-23	79.04	2.56	1.70	3.89	–	–	13.30	0.26	100.50
DAK-24	48.04	14.78	9.76	22.43	–	–	5.80	0.09	100.81
DAS50K-24	59.64	9.20	6.10	14.03	–	–	11.64	0.14	100.60
DAS100K-24	65.58	6.73	4.47	10.42	–	–	13.32	0.14	100.51
DAS400K-24	79.09	2.30	1.65	3.96	–	–	13.38	0.16	100.37
An-Di eutectic–SiO_2 system, samples enriched in Na and K									
DANK-26	48.28	14.90	9.84	22.47	2.98	0.06	2.62	0.07	101.10
DAS50NK-26	60.51	9.37	6.23	14.17	4.73	0.10	6.08	0.11	101.09
DAS100NK-26	66.65	6.89	4.56	10.39	5.05	0.11	7.42	0.09	100.97
DAS400NK-26	80.66	2.59	1.65	3.94	4.35	0.11	7.64	0.10	100.83
DANK-27	47.44	14.76	9.79	22.35	3.71	0.11	3.08	0.07	101.13
DAS25NK-27	53.54	11.93	7.92	17.98	4.85	0.07	4.94	0.05	101.16
DAS50NK-27	59.79	9.29	6.17	14.00	5.57	0.09	6.29	0.09	101.11
DAS100NK-27	65.89	6.97	4.55	10.38	5.78	0.10	7.59	0.09	101.15

Note: s.d. is one standard deviation.

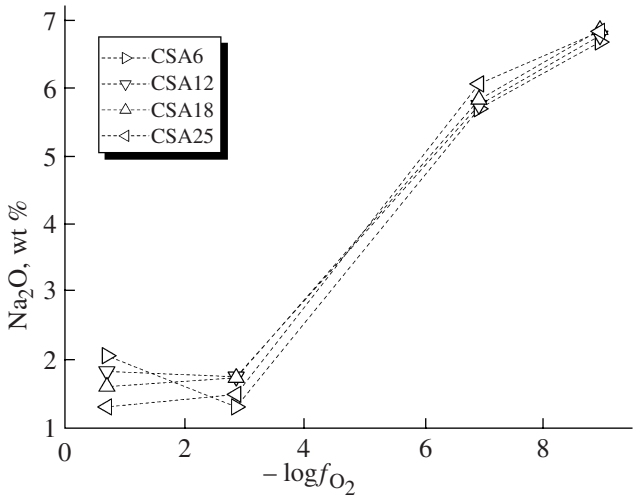

Fig. 2. Saturation of melts of CSA compositions ($Ca_2Si_3O_8$–Al_2O_3 system) with sodium as a function of oxygen fugacity.

the partial dissolution of the quartz crucible and alkali evaporation (Borisov et al., 2006). A question then arises as to whether the equilibrium content of alkalis can be determined in the experimental melts suspended in the crucible. The answer is probably yes. Despite the continuous variations in source melt composition, the experimental melts in loops are in dynamic equilibrium with this melt. By the example of Co-bearing melts, Borisov et al. (2006b) showed that starting Na-free and Na-rich melts placed simultaneously in a crucible with a Na-source melt had within error identical Na_2O contents after 20 h at 1400°C. Similarly, three Fe-bearing melts with different initial Na_2O contents showed similar Na_2O contents of 6.45 ± 0.14 wt % after a 4 h exposure. In both cases, the composition of the source melts shifted significantly toward higher SiO_2 contents, which did not prevent the equilibration of experimental melts in loops.

As was noted above, O'Neill (2005) used a similar method and showed that constant Na_2O contents in melts were reached within 8.5 h in experiments in air at 1400°C.

The rapid equilibration could be related to the convection in a melt contained in a wire loop (Borisov, 2001). Owing to this process, the surface layers saturated with alkalis through a vapor phase are constantly stirred by convection, which results in the homogeneous distribution of alkalis (according to microprobe analysis) and melt equilibration with the vapor phase with respect to alkali contents. The vapor phase may be in equilibrium with the source melt at a given time. In fact, the latter condition (vapor phase equilibrium with the composition of the source melt) is unimportant and, as will be shown below, unattainable. What is important is that all of the experimental melts occurring side by side in a crucible should be in equilibrium with the vapor phase. Even if the content of alkalis in this vapor phase is unknown, its equilibrium with all melts of the series allows us to determine the activity coefficients of Na_2O and K_2O in these melts, i.e., to estimate the influence of melt composition (if only within the given series) on the activity coefficients of alkalis.

Influence of Oxygen Fugacity on the Level of Melt Saturation with Alkalis

For the sake of brevity, the degree of experimental melt saturation with alkalis will hereafter be referred to as solubility, keeping in mind that the alkali solubility is determined in equilibrium with the vapor phase coexisting with the source melt under given T–f_{O_2} parameters rather than with the source melt.

The solubility of Na in similar melts is shown as a function of f_{O_2} in Fig. 2. Note that, in all of the experimental series presented in this diagram, the final compositions of the source melts were similar (22.1 ± 0.9 wt % Na_2O) and these experiments were conducted at identical temperatures and durations.

It can be seen that the transition from pure air ($\log f_{O_2}$ = –0.68) to pure CO_2 ($\log f_{O_2}$ = –2.84) is accompanied by negligible changes in Na solubility. In contrast, as the oxygen fugacity was further lowered (buffered by the CO/CO_2 gas mixture), the solubility of Na_2O increased rapidly. Thus, all other factors being equal, the solubility of Na_2O in a melt increases fourfold as f_{O_2} decreases by about 6 orders of magnitude.

It is clear that the level of melt saturation with alkalis can be controlled by varying the oxygen fugacity. This fact indicates that equilibrium between the experimental melts and the source melt was not attained. Indeed, the evaporation of Na from a melt can be described by the following reaction (Tsuchiyama et al., 1981)

$$NaO_{1/2}\ (\text{source}) = Na\ (\text{vapor}) + 1/4\ O_2\ (\text{vapor}). \quad (1)$$

On the other hand, the saturation of experimental melts with Na vapor can be described by a similar reaction,

$$Na\ (\text{vapor}) + 1/4O_2\ (\text{vapor}) = NaO_{1/2}\ (\text{experimental melt}). \quad (2)$$

Combining reactions (1) and (2) yields

$$NaO_{1/2}\ (\text{source}) = NaO_{1/2}\ (\text{experimental melt}). \quad (3)$$

Consequently, oxygen fugacity should play no role, and the degree of experimental melt saturation with alkalis at a given temperature must be fully controlled by the composition of the source or, more precisely, by the activity of alkalis in it. The dependence of Na_2O solubility in melts on f_{O_2} is most likely related to the kinetics of alkali evaporation from the source melt. Previously, O'Neill (2005) also observed an increase in Na_2O solubility in experimental melts at a decrease in

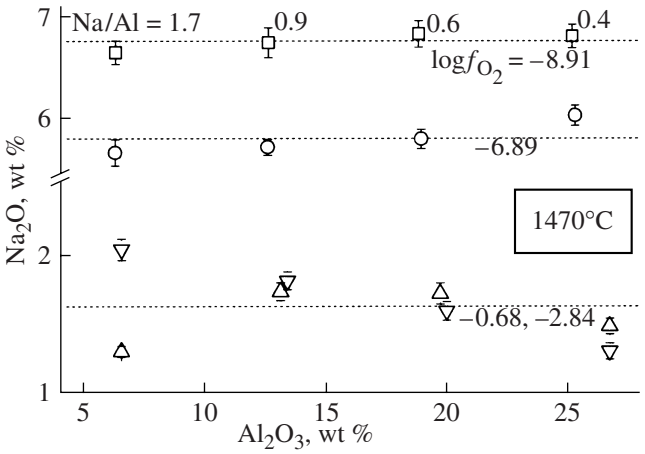

Fig. 3. Influence of Al_2O_3 content in CSA melts ($Ca_2Si_3O_8$–Al_2O_3 system) on the saturation of these melts with sodium. The dashed lines are average Na_2O contents for the given series ($\log f_{O_2}$ values are given). The series in air (up-pointing triangles) and pure CO_2 (down-pointing triangles) are combined together. For the most reduced series, which showed the widest range of atomic Na/Al ratios, the values of this ratio in experimental melts are shown.

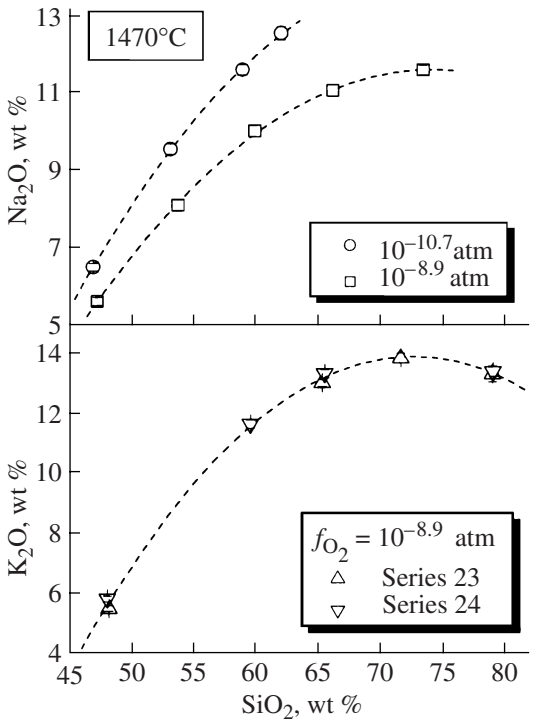

Fig. 4. Influence of SiO_2 content in DAS melts (*DiAn*–SiO_2 system) on the saturation of these melts with sodium and potassium.

f_{O_2} and suggested that this phenomenon has a kinetic origin.

Influence of Al_2O_3 on the Solubility of Alkalis in Silicate Melts

The solubility of Na_2O at a constant temperature of 1470°C in melts of the $2CaO \cdot 3SiO_2$–Al_2O_3 system is shown in Fig. 3. As can be seen from the diagram, the solubility of Na under the most reducing conditions ($10^{-8.9}$ atm) is independent of Al_2O_3 content within the experimental error. Under slightly more oxidizing conditions ($10^{-6.9}$ atm), the solubility of Na changes only slightly; however, there is a tendency toward a higher Na_2O solubility at higher Al_2O_3 content in the melt. Considerable variations in Na_2O solubility were observed in the oxidized experiments conducted in air or pure CO_2, which could be due to the very low Na partial pressure in the crucible and, as a result, incomplete equilibration of all of the experimental melts with the vapor phase. However, it is evident that even in this case Al_2O_3 content has a negligible effect on the Na solubility in melts.

Similar relations were observed in the single experimental series on the saturation of melts of the $2CaO \cdot 3SiO_2$–Al_2O_3 system with K_2O. The solubility of K_2O remained constant (5.8 wt %) within the limits of error as the Al_2O_3 content in the melt increased from 6 to 18 wt % and was slightly higher (6.4 wt %) only in the melt with 24 wt % Al_2O_3 (Table 3).

O'Neill studied the saturation of melts of the $CaMgSi_2O_6$–Al_2O_3 system with Na at 1400°C and also did not observe any significant influence of Al_2O_3 on Na_2O solubility (O'Neill, 2005, Fig. 3).

Thus, it can be concluded that, at any temperature and melt composition, alumina content has no significant influence on the solubility of alkalis in melts.

Influence of SiO_2 Content on Alkali Solubility

The effect of SiO_2 in the melts of the DA–SiO_2 system is illustrated in Figs. 4 and 5. It can be seen that, in contrast to Al_2O_3, SiO_2 exerts a significant influence on the solubility of alkalis and there are two specific features in the behavior of alkalis.

First, the solubility of alkalis increases rapidly as the SiO_2 content increases from 45 to 70 wt %. With respect to SiO_2 content, the model melts range from basaltic (DA) to dacitic (DAS100) compositions. Consequently, the partitioning of Na and K between the DAS100 and DA melts from a single series characterizes to a first approximation the dacite/basalt partition coefficients of D_{Na} or D_K. Averaging the data for various series yields $D_{Na} \approx 1.7$ and $D_K \approx 2.5$. These partition coefficients obtained by the analysis of physically separated melts are in essence similar to the transient equilibrium partition coefficients of alkalis between contacting felsic and basaltic melts (D_{Na} and D_K vary from 1.5 to 3.0; Watson, 1982; Watson and Jurewicz, 1984; Bindeman and Perchuk, 1993). It will be shown below that our data allow a more rigorous description of the

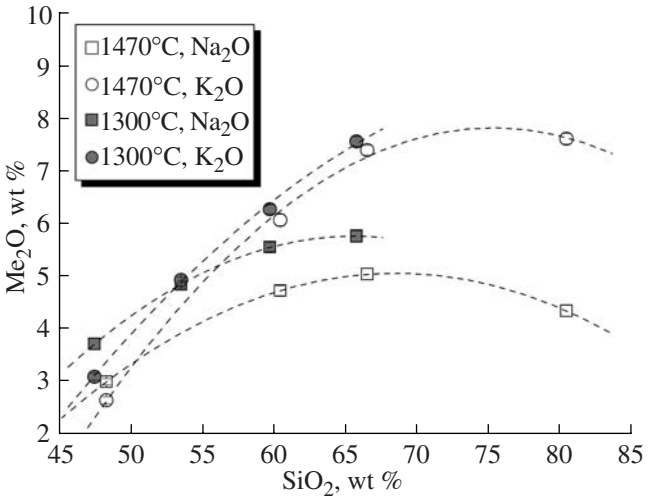

Fig. 5. Influence of SiO_2 content in DAS melts (*DiAn*–SiO_2 system) on the simultaneous saturation of these melts with sodium and potassium from a combined K–Na source.

dependence of D_{Na} and D_K on the difference in SiO_2 content between the coexisting melts.

The second important feature in the behavior of Na and K in the melts of the DA–SiO_2 system is the existence of a maximum of their solubility in silicic melts containing 66–76 wt % SiO_2 (Figs. 4, 5). Most of the curves pass through maxima at ~73–76 wt % SiO_2, and only the solubility of Na in experiments with combined K–Na sources shows maxima at lower SiO_2 contents of 66–69 wt %. In our previous investigations of the solubility of divalent metals in the melts of the DA–SiO_2 system (Borisov, 2006, 2007), we also observed maxima of Ni, Co, and Fe solubility, but they were confined to intermediate melt compositions (~55–59 wt % SiO_2), regardless of temperature, metal type, and metal content (from ppm levels to 13 wt %).

DISCUSSION

The weak dependence of the solubility of alkalis in melts on Al_2O_3 content is intriguing and calls for further experimental and theoretical investigations. Indeed, almost all theories of the structure of silicate melts postulate that alkalis are the most favorable network-modifying cations to compensate the charge of Al^{3+} in the tetrahedral position (structural groups of the $KAlO_2$ and $NaAlO_2$ type). This assumption is reflected in the calculation of the NBO/T parameter (nonbridging oxygen per tetrahedron) on the basis of the following order of preference of modifying cations for Al^{3+}: K^+, Na^+, Ca^{2+}, Mg^{2+}, etc. (e.g., Mysen, 1988). Hence, it could have been expected that the character of Na solubility in melts would change markedly when the molar Na_2O/Al_2O_3 ratio will be higher than 1. However, this is not the case; for instance, in the most reducing series in the $2CaO \cdot 3SiO_2$–Al_2O_3 system, the Na/Al atomic ratio varied from 1.75 to 0.45, whereas the solubility of Na in the melts was constant within errors (Fig. 3).

As was note by O'Neill (2005), who did not detect significant variations in Na solubility in the melts of the diopside–corundum join, this fact casts some doubt on the importance of the traditional boundary between agpaitic [Al/(Na + K) < 1] and metaluminous [Al/(Na + K) > 1] melts.

Note also that the similar behavior of K and Na in the melts of the CSA system is at odds with the choice of significantly different components for the thermodynamic description of K and Na oxides in some models of silicate melts (for instance, Na_2SiO_3 and $KAlSiO_4$ in the MELTS model or $NaSi_{0.5}O_{1.5}$ and $KAlSiO_4$ in pMELTS; Ghiorso et al., 2002).

Influence of SiO_2 content on the relative activity coefficients of Na_2O and K_2O in silicate melts. At least for simple binary Me_2O–SiO_2 systems, the activities of alkalis in the melt sources can be estimated from the available thermodynamic data (e.g., Charles, 1967; Rego et al., 1985). However, the absolute activity coefficients of alkalis in the experimental melts cannot be calculated. As was shown above, the dependence of the degree of saturation of experimental melts with alkalis on oxygen fugacity implies that the activities of Na_2O and K_2O in them are not identical to the activities of these alkalis in the source melts, with which they are in dynamic equilibrium. Nonetheless, the estimation of the relative activity coefficients of alkalis in the experimental melts may be instructive. Assuming that for each series the activities of Me_2O in all of the melts are identical and choosing one of the melts as a reference ($\gamma_{ref} = 1$), the activity coefficient of Me_2O in melt i can be expressed as $\gamma_i = (X_{Me_2O})_{ref}/(X_{Me_2O})_i$. In order to unify all of the series, a virtual melt with $X_{SiO_2} = 0.45$ was selected as a common reference. The $(X_{Me_2O})_i$ value of the reference melt was determined for each series by extrapolating data for all samples of this series. The calculated γ_i values are shown in Table 4 and Fig. 6 as a function of SiO_2 content in the melt.

Similar to the case of solubility (Figs. 4, 5), there are two characteristic features in the dependence of the activity coefficients of alkalis on silica content in the melt.

First, the γ_{Na_2O} and γ_{K_2O} values decrease rapidly as the X_{SiO_2} increases from 0.45 to 0.70, and the decrease of γ_{K_2O} is more significant (on average, from 1.0 to 0.3) than that of γ_{Na_2O} (on average, down to 0.5).

Second, there is a minimum of γ_i at X_{SiO_2} between 0.66 and 0.76. The minimum of γ_{Na_2O} is more pronounced and shifted toward more basic compositions compared with that of γ_{K_2O} (Fig. 6). In the melts of the

same system (DA–SiO_2), we previously detected minima of γ_{NiO}, γ_{CoO}, and γ_{FeO} at intermediate melt compositions (X_{SiO_2} from 0.55 to 0.59) (Borisov, 2006, 2007).

The minima of the activity coefficients (solubility maxima) of alkalis suggest that silicic melts must not always be enriched in alkalis relative to less silicic melts. The analysis of the published compositions of coexisting liquids in systems with liquid immiscibility supports this suggestion. Although alkalis are typically enriched in more silicic melts (Watson, 1976; Ryerson and Hess, 1978), the opposite relations are also possible. For instance, in complex immiscible melts of the SiO_2–TiO_2–Al_2O_3–FeO–MgO–CaO–Na_2O system, very silicic liquids (up to 92.3 wt % SiO_2) are depleted in Na compared with less silicic melts (Hess and Wood, 1982, Table 2).

The minima of the activity coefficients of alkalis in binary Me_2O–SiO_2 systems (Me = Li, K, or Na) at X_{SiO_2} from 0.7 to 0.9 were found by Charles (1967, Figs. 4, 12, 20). However, it should be noted that the γ_{Me_2O} values were estimated by the numerical integration of the Gibbs–Duhem equation, and the γ_{SiO_2} values that were used for this purpose were obtained from appropriate phase diagram using the cryoscopic equation (Charles, 1967). Since direct experimental data were used in our case (although they are shown in Fig. 6 as relative activity coefficients), the existence of γ_{Me_2O} minima is beyond doubt. We believe that the γ_{Me_2O} minima reported by Charles (1967) are real rather than artifacts of the calculation method.

Uphill diffusion: where and when it can be expected. The principles and mechanisms of uphill diffusion, i.e., movement of component N against the gradient of its concentration (C_N), were discussed in detail by Zhang (1993). We will follow the simplest interpretation postulating that N always diffuses down its chemical potential (μ_N) gradient (Sato, 1975; Watson and Jurewicz, 1984). If two contacting melts (A and B) with different degrees of nonideality have $\mu^A > \mu^B$ but $C^A < C^B$, component N will diffuse from melt A to melt B, providing an example of uphill diffusion. It is evident that when basic and silicic melts at identical temperatures and with approximately equal amounts of alkalis (in particular, this is characteristic of sodium) are brought into contact, alkalis will always diffuse from the basic into silicic melt. If the contents of alkalis in the silicic melt is initially much higher than those in the basic melt (which is more typical of potassium), the nature of diffusion (uphill or downhill) can be predicted on the basis of a comparison of the activity coefficients γ_{Me_2O} in the coexisting melts. Since the activities a^A and a^B must be equal at equilibrium, component N will diffuse from melt A to melt B, if $X^A/X^B > \gamma^B/\gamma^A$, and in the opposite direction, if $X^A/X^B < \gamma^B/\gamma^A$.

Table 4. Thermodynamic characteristics of melts of the *An-Di* utectic–SiO_2 system

Sample	X_{SiO_2}	X_{Na_2O}	X_{K_2O}	γ_{Na_2O}	γ_{K_2O}
Samples enriched in Na					
Standard 8	0.450	0.055	0.000	1.000	–
DANa-8	0.468	0.063	0.000	0.873	–
DAS25Na-8	0.529	0.092	0.000	0.595	–
DAS50Na-8	0.590	0.112	0.000	0.487	–
DAS70Na-8	0.618	0.121	0.000	0.452	–
Sandard 13	0.450	0.047	0.000	1.000	–
DANa-13	0.473	0.054	0.000	0.871	–
DAS25Na-13	0.538	0.078	0.000	0.603	–
DAS50Na-13	0.601	0.097	0.000	0.487	–
DAS100Na-13	0.665	0.107	0.000	0.440	–
DAS200Na-13	0.736	0.112	0.000	0.421	–
Samples enriched in K					
Standard 23	0.450	0.000	0.027	–	1.000
DAK-23	0.485	0.000	0.035	–	0.771
DAS100K-23	0.682	0.000	0.087	–	0.313
DAS200K-23	0.753	0.000	0.093	–	0.292
DAS400K-23	0.826	0.000	0.089	–	0.305
Standard 24	0.450	0.000	0.029	–	1.000
DAK-24	0.485	0.000	0.037	–	0.771
DAS50K-24	0.617	0.000	0.077	–	0.375
DAS100K-24	0.684	0.000	0.089	–	0.325
DAS400K-24	0.827	0.000	0.089	–	0.323
Samples enriched in Na and K					
Standard 26	0.450	0.024	0.013	1.000	1.000
DANK-26	0.481	0.029	0.017	0.847	0.759
DAS50NK-26	0.612	0.046	0.039	0.526	0.323
DAS100NK-26	0.678	0.050	0.048	0.489	0.263
DAS400NK-26	0.824	0.043	0.050	0.567	0.255
Standard 27	0.450	0.032	0.016	1.000	1.000
DANK-27	0.473	0.036	0.020	0.885	0.833
DAS25NK-27	0.538	0.047	0.032	0.671	0.515
DAS50NK-27	0.605	0.055	0.041	0.581	0.402
DAS100NK-27	0.670	0.057	0.049	0.557	0.331

Note: The activity coefficients of alkalis were calculated relative to a reference melt with $X_{SiO_2} = 0.45$. The X_{Na_2O} and X_{K_2O} values in the standard glasses were obtained by the extrapolation of alkali contents to $X_{SiO_2} = 0.45$.

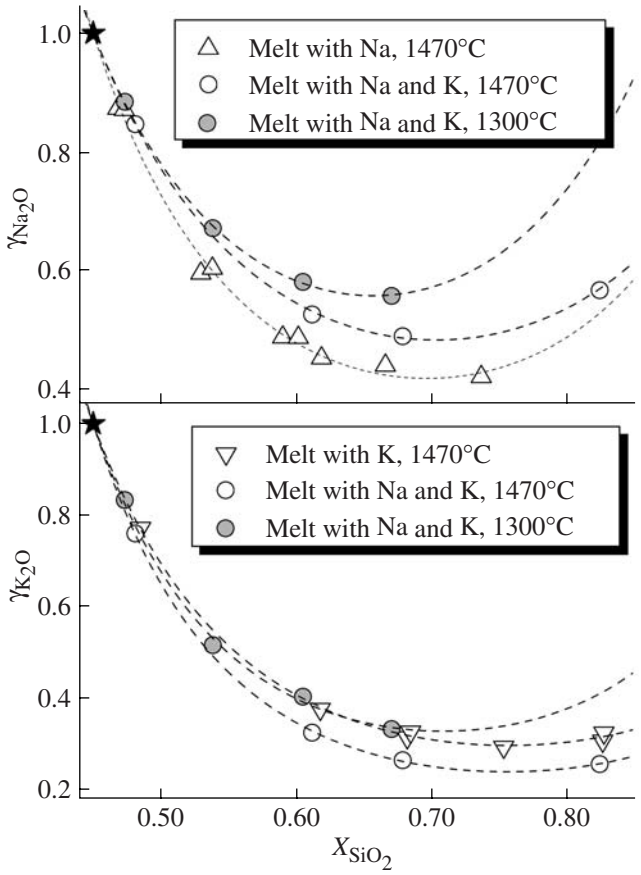

Fig. 6. Influence of X_{SiO_2} on the activity coefficients of Na_2O and K_2O in DAS melts (*DiAn*–SiO_2 system). γ_{Na_2O} and γ_{K_2O} in melts with X_{SiO_2} = 0.45 are taken to be 1 (compositions are shown by asterisks). See text for calculation details.

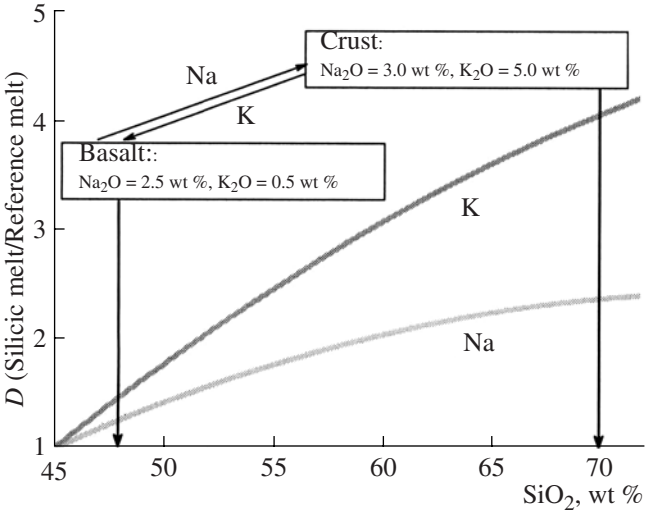

Fig. 7. Relative enrichment of alkalis in melts more silicic than the reference melt with 45 wt % SiO_2. Also shown are the compositions of the basic and silicic melts selected for further calculations.

As was noted above, a similar approach was previously proposed by Watson (1982), who introduced the transient partition coefficients of alkalis between felsic and basaltic melts. When the C^A/C^B ratio for Na or K is lower than the equilibrium value of $D^{A/B}$, the component will diffuse from melt A into melt B.

Crustal contamination of basic melts and evolution of silicic xenoliths in basic magmas. Common sense suggests that basic magmas must be affected by crustal contamination en route to the surface from their generation zones in the continental mantle. In the simplest case, basic melts assimilate the wall rocks of magma conduits and reservoirs and/or silicic liquids produced by partial melting of crustal material at the contact with the basic magmas. More sophisticated models should involve alkali redistribution between silicic and basic melts, because the diffusion rate of alkalis in silicate melts is probably several orders of magnitude higher than the diffusion rate of other components (e.g., Watson, 1982). The extreme case is the perfectly mobile behavior of Na and K during contamination at the inert behavior of other major elements. The volume of basic melt can be considered limited compared with the volume of the crust, which is treated as infinite.

Another example of contamination is silicic melts in crustal xenoliths immersed in an infinite volume of basic magma. In this case, we also can consider both simple mixing of silicic and basic melts in varying proportions and perfectly mobile behavior of alkalis coupled with the inert behavior of other components.

In order to construct numerical models of contamination/mixing, the compositions of silicic and basic melts and Na and K partition coefficients between them should be specified. Let us assume that the basic melt contains 48 wt % SiO_2, 2.5 wt % Na_2O, and 0.5 wt % K_2O. These contents are close to the average chemical composition of basalts from oceanic and continental areas (*Igneous Rocks,* 1983). The average composition of the upper continental crust was recently estimated by Rudnick and Gao (2003): 66.6 wt % SiO_2, 3.3 wt % Na_2O, and 2.8 wt % K_2O. However, partial melts derived from gneisses and granulites may be much more silicic and potassic: up to 74 wt % SiO_2 and 6.4 wt % K_2O (Beard et al., 1993). To unify the calculations, let us assume that the silicic composition contains 70 wt % SiO_2, 3 wt % Na_2O, and 5 wt % K_2O, be it an initial rock or partial melt.

As can be seen in Figs. 4 and 5, the partition coefficients of Na and K between basic and silicic melts depend on the SiO_2 contents of the melts. Using a basic melt with 45 wt % SiO_2 as a reference, the relative alkali enrichment (D) of more silicic melts can be described by the quadratic equation

$$D_{Me_2O} = a(C_{SiO_2} - 45) + b(C_{SiO_2} - 45)^2 + 1, \quad (4)$$

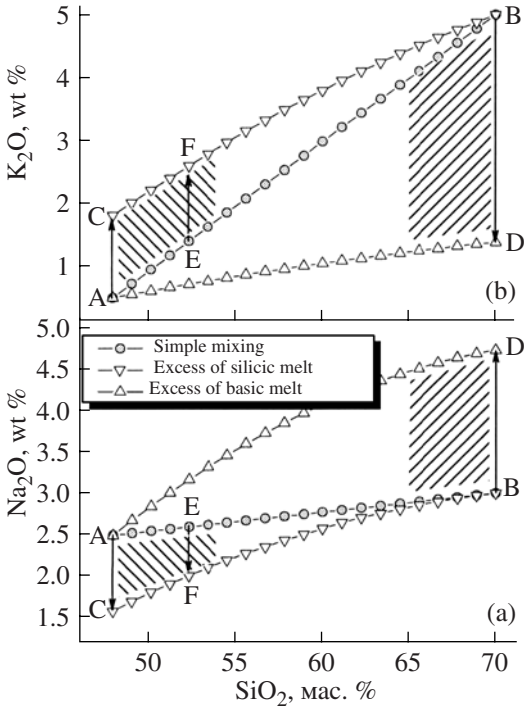

Fig. 8. Behavior of (a) Na and (b) K during the mixing/contamination of basic and silicic melts. See text for calculation details.

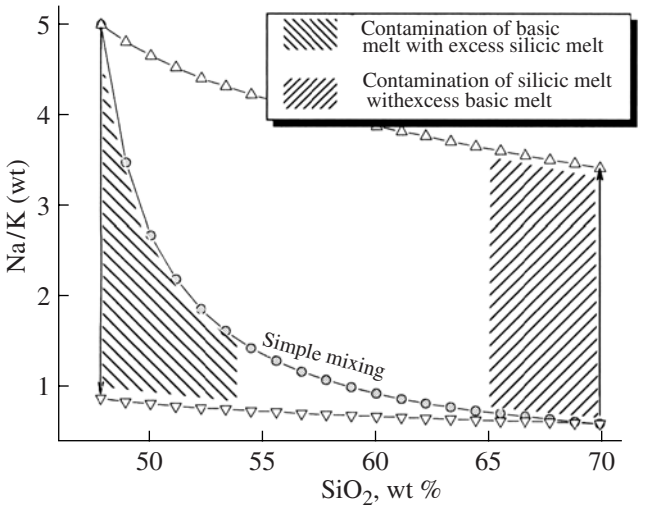

Fig. 9. Dependence of the Na/K ratio on SiO_2 content during the mixing/contamination of basic and silicic melts. See text for calculation details.

where C_{SiO_2} is the SiO_2 content in wt %; and a and b are 0.0923 and –0.00147 for Na and 0.1627 and –0.00158 for K, respectively. This equation was based on all of the experimental data regardless of temperature, except for a few of the most silicic melts falling far beyond the maxima of alkali solubility in Figs. 4 and 5. The calculated R^2 values are 0.89 for D_{Na} and 0.91 for D_K. Equation (4) can be used to estimate the partition coefficients of alkalis between two coexisting melts, A and B, $D^{A/B} = C^A/C^B$.

Figure 7 shows the curves of relative alkali enrichment in melts as a function of SiO_2 content, which were calculated using Eq. (4), and the compositions of basic (basalt) and silicic (crust) melts accepted in our modeling. Equation (4) yields $D_{Na} = 1.9$ and $D_K = 2.8$ for these melts, i.e., the uphill diffusion of sodium from the basic to the silicic melt and the normal diffusion of potassium from the silicic to the basic melt should be expected for the accepted alkali contents.

The model of mixing and contamination of melts is illustrated in Fig. 8. The curve AB corresponds to the simple mixing of varying amounts of basic and silicic melts. However, given the perfectly mobile behavior of alkalis and infinite volume of silicic material, the basic melt (point A) can lose part of its Na and gain a significant amount of K (arrows AC). A combination of the perfectly mobile and inert behavior of alkalis can be simulated in the following manner: a melt lying on the mixing line AB (for instance, E) interacts with an infinite amount of silicic melt, which leads to its enrichment in Na and depletion in K (point F). Note that the CD curves correspond to the complete equilibration of contaminated melt with the excess amount of silicic liquid. However, equilibrium may be not attained or the amount of silicic liquid (source of Na and sink for K) may be limited. This implies that, in the most general case, the composition of contaminated melt can lie anywhere within the ABC segment, but most likely near the line AC. These melts are arbitrarily limited in Fig. 8 by an SiO_2 content of 54 wt % and marked by hatching.

Similarly, the composition of silicic melts in crustal xenoliths immersed in an infinite volume of basic magma must occur in the segment ABD, but most likely in the region adjacent to the line BD. These melts are arbitrarily limited by an SiO_2 content of 65 wt % and marked by hatching in Fig. 8.

The presented model of mixing/contamination ignores kinetic problems, possible difference in temperature between the mixed melts, and the crystallization of mineral phases and their possible assemblages at the perfectly mobile behavior of alkalis (e.g., Zharikov, 1999). This model does not claim to comprehensively describe natural processes, but, rather, it is intended to demonstrate the possibility of the formation of rocks with wide variations in alkali contents at relatively minor variations in SiO_2.

Note finally that the perfectly mobile behavior of alkalis must result in the potassic specifics of basalts affected by crustal contamination and, correspondingly, the sodic specifics of silicic melts in crustal xenoliths

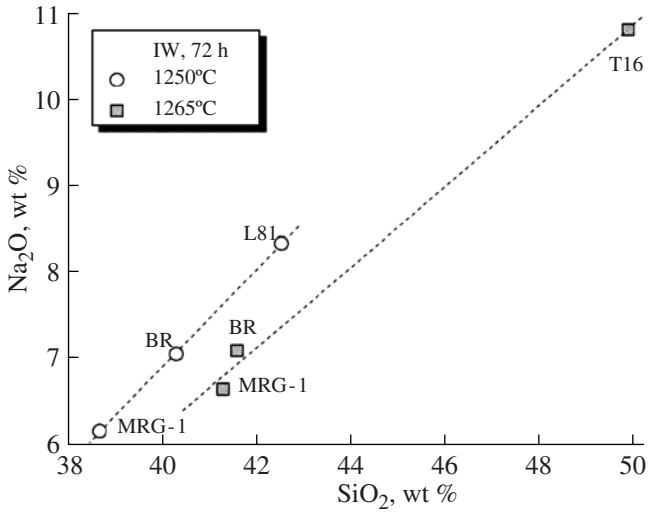

Fig. 10. Example of the influence of SiO_2 content in natural basic and ultrabasic melts on their saturation with sodium. BR is the standard basalt (MgO content in the bulk rock is 13.3 wt %, and that in melts at 1250 and 1265°C, 10.3 and 12.0 wt %, respectively); MFR-1 is the standard gabbro (MgO content in the bulk rock is 13.6 wt %, and that in melts at 1250 and 1265°C, 10.1 and 12.1 wt %, respectively); L81 is the ultrabasic composition provided by A.A. Gurenko (MgO contents in the bulk rock and glass are 20.2 and 10.1 wt %, respectively); and T16 is the basalts of the Great Fissure Tolbachik Eruption, Kamchatka (10.9 wt % MgO). All of the melts, except for T16, contained olivine as a liquidus phase at experimental temperature.

contaminated with the enclosing basaltic melt. This is clearly seen in Fig. 9, which shows the Na/K ratio of the melts considered above.

Possibility of alkali redistribution between samples in loop experiments. At first glance, this topic seems to be trifling in general petrology. However, it is intimately related to the problems of the elucidation of the shortcomings and advantages and development of the loop technique, which has become a standard in petrological and geochemical investigations at a total pressure of 1 atm (Donaldson et al., 1975; Corrigan and Gibb, 1979; Grove, 1981; Borisov and Jones, 1999; Borisov, 2001; O'Neill, 2005; Borisov et al., 2006).

It is known that alkali exchange between high- and low-alkali melt occurring side by side in a furnace is observed even in classic loop experiments (i.e., without an additional source melt) (e.g., Borisov et al., 2006, p. 768). The experiments of O'Neill (2005) with DA–Na_2SiO_3 melts are instructive in this respect. Given the perfectly mobile behavior of sodium in such experiments, the DA–Na_2SiO_3 system is equivalent to the DA–SiO_2 system, which was studied by us. After 118 h annealing at 1400°C and $f_{O_2} = 10^{-12}$ atm, the Na_2O content in glasses increased by a factor of almost two as SiO_2 increased from 50 to 57 wt % (O'Neill, 2005, Fig. 3).

The above considerations add one more limitation to the classic loop technique [the first limitation being the significant loss of alkalis under reducing conditions (Donaldson et al., 1975; Corrigan and Gibb, 1979; Borisov et al., 2006)]. Although the loop technique allows one to suspend several samples in the hot zone of a furnace [at least up to eight samples (Doyle and Naldrett, 1986)], the investigation of basic and silicic melts in a single run should be avoided. Otherwise, in addition to the simple loss of alkalis, their redistribution between samples with different SiO_2 contents can be expected. If the focus of the study is the crystallization sequence of melts, the partition of alkalis into silicic melts can lead to changes in liquidus temperatures and phase relations.

The same is true of more basic melts. The author recently employed the crucible supported loop technique to study the influence of Na on Fe–Mg partitioning between olivine and melt. The results of these experiments will be reported in a special publication, and here we only show some data on the saturation of basic and ultrabasic natural melts with Na. As an example, Fig. 10 shows two series of three samples each with different SiO_2 contents. All of the samples, except for T16, contain olivine. The influence of SiO_2 on melt saturation with Na is evident in each series. For instance, it was found that an increase in SiO_2 content from 41 to 50 wt % at 1265°C results in an increase in Na_2O content from 6.6 to 10.8 wt %, i.e., by more than 60% rel. In other words, the above restriction to the loop technique must be even stronger: any melts with different SiO_2 contents (from ultrabasic to silicic) exposed in a single melting experiment may undergo alkali redistribution through a vapor phase.

CONCLUSIONS

The saturation of silicate melts of varying Al_2O_3 and SiO_2 contents with alkalis was studied at a total pressure of 1 atm and temperatures of 1300–1470°C using the crucible supported loop technique.

It was shown that Al_2O_3 content has a negligible influence on the degree of K and Na saturation in silicate melts. In contrast, SiO_2 variations significantly affect the solubility of alkalis in silicate melts.

Model calculations showed that the perfectly mobile behavior of alkalis must lead to a potassium specifics in basalts contaminated by crustal materials and, correspondingly, a sodic affinity in silicic melts from crustal xenoliths contaminated by the enclosing basaltic melt.

ACKNOWLEDGMENTS

The author thanks L.L. Perchuk (Moscow State University) and L.Ya. Aranovich (Institute of Geology of Ore Deposits, Petrography, Mineralogy, and Geochemistry, Russian Academy of Sciences) for critical comments, which resulted in a considerable improvement of the manuscript. This study was financially supported by the Deutsche Forschungsgemeinschaft (DFG), the Russian Foundation for Basic Research, priority research programs of the Division of Earth Sciences of the Russian Academy of Sciences, and Russian President's Program for the support of leading scientific schools.

REFERENCES

1. J. S. Beard, R. J. Abitz, and G. E. Lofgren, "Experimental Melting of Crustal Xenoliths from Kilbourne Hole, New Mexico and Implications for the Contamination and Genesis of Magmas," Contrib. Mineral. Petrol. **115**, 88–102 (1993).
2. I. N. Bindeman and L. Perchuk, "Experimental Studies of Magma Mixing," Int. Geol. Rev. **35**, 721–738 (1993).
3. A. Borisov, "Loop Technique: Dynamic of Metal/Melt Equilibration," Mineral. Petrol. **71**, 87–94 (2001).
4. A. Borisov, "Experimental Study of the Effect of SiO_2 on Ni Solubility in Silicate Melts," Petrologiya **14**, 564–575 (2006) [Petrology **14**, 530–539 (2006)].
5. A. Borisov, "Experimental Study of the Influence of SiO_2 on the Solubility of Cobalt and Iron in Silicate Melts," Petrologiya **15**, 563–570 (2007) [Petrology **15**, 523–529 (2007)].
6. A. Borisov and J. H. Jones, "An Evaluation of Re, as an Alternative for Pt, for 1-bar Loop Technique: An Experimental Study at 1400°C," Am. Mineral. **84**, 1258–1534 (1999).
7. A. Borisov, Y. Lahaye, and H. Palme, "The Effect of Sodium on the Solubilities of Metals in Silicate Melts," Am. Mineral. **91**, 762–771 (2006).
8. N. L. Bowen, *The Evolution of the Igneous Rocks* (Princeton University Press, Princeton, 1928).
9. R. J. Charles, "Activities in Li_2O–, Na_2O– and K_2O–SiO_2 Solutions," J. Am. Ceram. Soc. **12**, 631–641 (1967).
10. G. Corrigan and F. G. F. Gibb, "The Loss of Fe and Na from a Basaltic Melt during Experiments Using the Wire-Loop Method," Mineral. Mag. **43**, 121–126 (1979).
11. P. S. Deines, R. H. Nafziger, G. C. Ulmer, and E. Woermann, "Temperature–Oxygen Fugacity Tables for Selected Gas Mixtures in the System C–H–O at One Atmosphere Total Pressure," Bull. Earth Miner. Sci., Experimental Station., No. 88 (1974).
12. C. H. Donaldson, R. J. Williams, and G. Lofgren, "A Sample Holding Technique for Study of Crystal Growth in Silicate Melts," Am. Mineral. **60**, 324–326 (1975).
13. C. Doyle and A. J. Naldrett, "Ideal Mixing of Divalent Cations in Mafic Magma and Its Effect on the Solution of Ferrous Oxide," Geochim. Cosmochim. Acta **50**, 435–443 (1986).
14. M. S. Ghiorso, M. M. Hirschmann, P. W. Reiners, and V. C. Kress, "The pMELTS: A Revision of MELTS for Improved Calculation of Phase Relations and Major Element Partitioning Related to Partial Melting of the Mantle to 3 GPa," Geochem. Geophys. Geosyst. **3**, 10.1029/2001GC000217 (2002).
15. T. L. Grove, "Use of FePt Alloys to Eliminate the Iron Loss Problem in 1 Atmosphere Gas Mixing Experiments: Theoretical and Practical Considerations," Contrib. Mineral. Petrol. **78**, 298–304 (1981).
16. P. C. Hess and M. I. Wood, "Aluminum Coordination in Metaaluminous and Peralkaline Silicate Melts," Contrib. Mineral. Petrol. **81**, 103–112 (1982).
17. D. A. Johnston and P. J. Wyllie, "Interaction of Granitic and Basic Magmas: Experimental Observations on Contamination Processes at 10 kbar with H_2O," Contrib. Mineral. Petrol. **98**, 352–362 (1988).
18. A. Kouchi and I. Sunagawa, "A Model for Mixing Basaltic and Dacitic Magmas as Deduced from Experimental Data," Contrib. Mineral. Petrol. **89**, 17–23 (1985).
19. *Igneous Rocks. Classification, Nomenclature, Petrography* (Nauka, Moscow, 1983) [in Russian].
20. B. O. Mysen, *Structure and Properties of Silicate Melts* (Elsevier, Amsterdam, 1988).
21. H. Nekvasil, A. Dondolini, J. Horn, et al., "The Origin and Evolution of Silica-Saturated Alkalic Suites: An Experimental Study," J. Petrol. **45**, 693–721 (2004).
22. H. St. C. O'Neill, "A Method for Controlling Alkali-Metal Oxide Activities in One-Atmosphere Experiments and Its Application to Measuring the Relative Activity Coefficients of $NaO_{0.5}$ in Silicate Melts," Am. Mineral. **90**, 497–501 (2005).
23. D. N. Rego, G. K. Sigworth, and W. O. Philbrook, "Thermodynamic Study of Na_2O–SiO_2 Mets at 1300°C and 1400°C," Metallurg. Trans. **16B**, 313–323 (1985).
24. R. Rudnick and S. Gao, "Composition of the Continental Crust," in *Treatise on Geochemistry* (Elsevier, Oxford, 2003), Vol. 3, pp. 1–64.
25. F. J. Ryerson and P. C. Hess, "Implications of Liquid–Liquid Distribution Coefficients to Mineral–Liquid Par-

titioning," Geochim. Cosmochim. Acta **42**, 921–932 (1978).

26. H. Sato, "Diffusion Coronas around Quartz Xenocrysts in Andesite and Basalts from Tertiary Volcanic Region in Northeastern Shikoku, Japan," Contrib. Mineral. Petrol. **50**, 46–64 (1975).
27. C. S. J. Shaw, Y. Thibault, A. D. Edgar, and F. E. Lloyd, "Mechanisms of Orthopyroxene Dissolution in Silica-Undersaturated Melts at 1 Atmosphere and Implications for the Origin of Silica-Rich Glass in Mantle Xenoliths," Contrib. Mineral. Petrol. **132**, 354–370 (1998).
28. A. Tsuchiyama, H. Nagahara, and I. Hushiro, "Volatilization of Sodium from Silicate Melt Spheres and Its Application to the Formation of Chondrules," Geochim. Cosmochim. Acta **45**, 1357–1367 (1981).
29. I. V. Veksler, A. M. Dorfman, L. V. Danyushevsky, et al., "Immiscible Silicate Liquid Partition Coefficients: Implications for Crystal–Melt Element Partitioning and Basalt Petrogenesis," Contrib. Mineral. Petrol. **152**, 685–702 (2006).
30. E. B. Watson, "Two-Liquid Partition Coefficients: Experimental Data and Geochemical Implications," Contrib. Mineral. Petrol. **56**, 119–134 (1976).
31. E. B. Watson, "Basalt Contamination by Continental Crust: Some Experiments and Models," Contrib. Mineral. Petrol. **80**, 73–87 (1982).
32. E. B. Watson and S. R. Jurewicz, "Behaviour of Alkalis during Diffusive Interaction of Granitic Xenoliths with Basaltic Magma," J. Geol. **92**, 121–131 (1984).
33. H. S. Yoder, Jr., "Contemporaneous Basaltic and Rhyolitic Magmas," Am. Mineral. **58**, 153–171 (1973).
34. Y. Zhang, "A Modified Effective Binary Diffusion Model," J. Geophys. Res. **98**, 11901–11920 (1993).
35. V. A. Zharikov, "Effects of Alkali Regimes on the Parageneses of Igneous Rocks," Petrologiya **7**, 340–355 (1999) [Petrology **7**, 324–338 (1999)].